


Review

# Principles of Dispersing Powders for 3D Printing

Hongli Zhou<sup>1</sup>, Xiaofeng Wang<sup>1,2,\*</sup> , Xinyu Wang<sup>1</sup>, Chaoqun Peng<sup>1</sup>, Richu Wang<sup>1</sup> and Kechao Zhou<sup>2</sup>

<sup>1</sup> School of Materials Science and Engineering, Central South University, Changsha 410083, China; summertimezhl@163.com (H.Z.); zndxwxy@csu.edu.cn (X.W.); pcq2005@163.com (C.P.); wrc910103@163.com (R.W.)

<sup>2</sup> State Key Laboratory of Powder Metallurgy, Central South University, Changsha 410083, China; zhoukc2@csu.edu.cn

\* Correspondence: wangxiaofeng@csu.edu.cn; Tel.: +86-134-6751-6329

**Abstract:** During the past 30 years, more and more 3D-printing techniques based on suspensions with specific rheological properties have been innovated and improved. In this review, principles of dispersing and controlling powders for suspension-based 3D printing are summarized. The suspensions for direct ink writing (DIW) are taken as an example for 3D printing. According to the rheological property requirement of suspensions for direct ink writing, the routes on how its rheological properties can be manipulated are summarized and classified into two categories: I. self-solidification route; II. assistant-solidification route. The perspective on the future of 3D-printing techniques based on suspensions is also discussed.

**Keywords:** suspensions; dispersing; powder; particles; 3D printing; rheological properties; direct ink writing



**Citation:** Zhou, H.; Wang, X.; Wang, X.; Peng, C.; Wang, R.; Zhou, K. Principles of Dispersing Powders for 3D Printing. *Colloids Interfaces* **2021**, *5*, 25. <https://doi.org/10.3390/colloids5020025>

Academic Editor:  
Alexander Kamyshny

Received: 16 January 2021  
Accepted: 11 March 2021  
Published: 14 April 2021

**Publisher's Note:** MDPI stays neutral with regard to jurisdictional claims in published maps and institutional affiliations.



**Copyright:** © 2021 by the authors. Licensee MDPI, Basel, Switzerland. This article is an open access article distributed under the terms and conditions of the Creative Commons Attribution (CC BY) license (<https://creativecommons.org/licenses/by/4.0/>).

## 1. Introduction

During the past three decades, 3D printing (additive manufacturing), preparing 3D objects in a layer-by-layer approach, has been dramatically developed from organic, metallic, to ceramic materials for wide applications in academia, industry, and daily life [1–8].

A variety of 3D-printing techniques are innovated and improved, which can be classified into seven categories: binder jetting, directed energy deposition, material extrusion, material jetting, powder bed fusion, sheet lamination, and vat photopolymerization, according to the stand of the International Organization for Standardization (ISO)/American Society for Testing and Materials (ASTM) 52,900:2015. Interestingly, several techniques among these are based on suspensions (slurries) with aspecific rheological properties, i.e., the materials are in the form of suspensions for undergoing 3D printing [5,9–15].

Selective laser sintering belonging to directed energy deposition is applied to fabricate high-strength alumina parts with high solid loading (~50 vol%) alumina suspension [9]. Stereolithography apparatus (SLA)/digital light processing (DLP) [5] belonging to vat photopolymerization are used to print ceramic parts such as silica (SiO<sub>2</sub>) [10–13,16,17], zirconia (ZrO<sub>2</sub>) [18], hydroxyapatite (HA) [19], and silicon nitride (Si<sub>3</sub>N<sub>4</sub>) [10]. Based on suspensions, direct ink writing (DIW) belonging to material extrusion, pioneered by Lewis [20] and Cesarano [21], is used in the fabrication of three-dimensional structures, including polyelectrolytes [22], ceramics [20,23], aerogels [24], etc. No matter what 3D-printing technique based on suspensions is performed, the key to successful printing is the preparation of suspensions whose properties should fulfill the requirements of the forming techniques. That is, dispersing of powders in a solvent and controlling the rheological properties are the most important points. Therefore, it is necessary to understand the principles of dispersing powder and to clarify routes for tailoring the properties of suspensions.

The purpose of this paper is to review dispersing and controlling of powders for suspension-based 3D printing. Particular emphasis is given to routes made in recent decades, especially for direct ink writing. Firstly, to support the underlying concepts, the basic theory of dispersing powder in a solvent is briefly introduced, including tailoring suspension rheological properties by adjusting interparticle interactions. Then, the suspensions for DIW are taken as an example. According to the property requirement of suspensions for direct ink writing, the routes on how its rheological properties can be manipulated are summarized and divided into two types: I. self-solidification route; II. assistant-solidification route. Finally, the perspective on the future of 3D-printing techniques based on suspensions is discussed.

## 2. Basic Theory of Dispersing Powder

As aforementioned, each of the 3D-printing techniques discussed in this paper begins with suspensions possessing various rheological properties as the starting state. It is, therefore, critical to understand how powder particles suspending in its solvent can be dispersed as well as adjusted, i.e., how particle interaction in determining suspension rheology for the chosen printing technique can be tailored. Typically, there are three states of particle interaction in suspensions: well-dispersed, weakly aggregated, and strongly aggregated, as illustrated in Figure 1 [25–30]. These results stemmed from the interparticle forces in the dispersing system, including attractive forces such as the van der Waals and repulsive forces such as electrostatic (double layer) and steric (polymer-induced) forces. As repulsive forces dominate, particle interaction in suspensions is in the well-dispersed state. As attractive forces dominate but not very high, particle interaction is in the weakly aggregated state, and thus, either isolated clusters in suspension at lower volume fractions or a particle network at higher volume fractions are formed. As attractive forces dominate and are very high, particle interaction is in the strongly aggregated state, and thus, either a touching particle network or individual clusters in suspension, depending on their volume fractions, are formed. In this section, we will provide a brief account of the theories underlying each of these forces to understand how one may manipulate forces of particle interaction to tailor states of particle interaction and then to generate the desired rheological properties of suspensions, with examples of applications in 3D printing.

### 2.1. Interparticle Forces

No matter what intervening solvent (aqueous or organic) is used to suspend powder, there is a ubiquitous force between particles of the same materials, called van der Waals (vdW). vdW is a long-range, attractive force that exhibits a power-law distance dependence, and its strength depends on the dielectric properties of the particle's materials and solvent [26,27]. There are few ways to adjust this force and manipulate suspension properties [31,32] to be suitable for forming processes. Because the dielectric properties are a natural instinct of materials, one approach, that is, by matching the particles and solvent, can be used to tailor this force [31,32]. However, this approach is of limited practical application. Therefore, triggering the interaction repulsion between particles such as electrostatic and steric forces, as shown in Figure 1, is a critical approach to adjust interaction force, states of particle interaction, and rheological properties of suspensions for 3D printing.

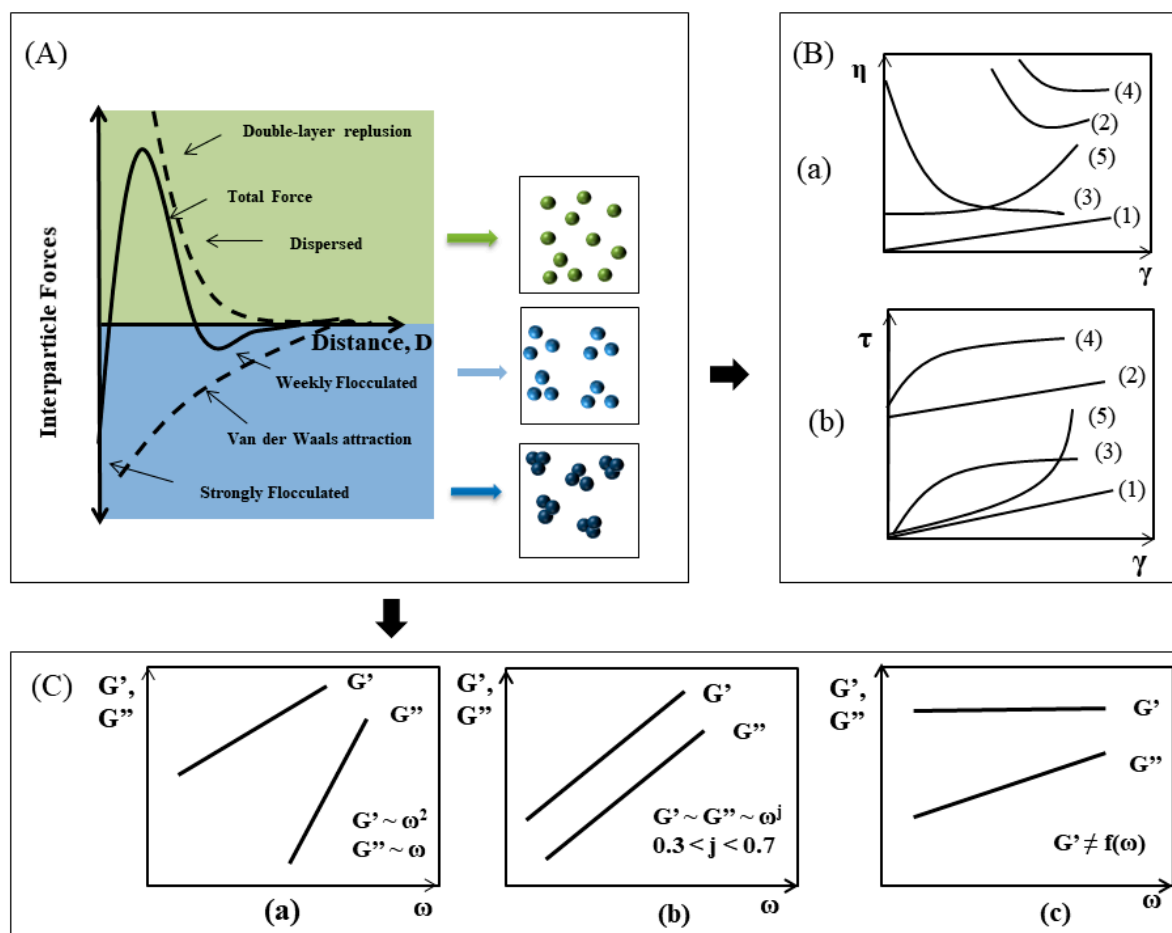


**Figure 1.** (A) Schematic illustration of the interparticle force as a function of the distance between particles. The force is a function of the distance ( $D$ ) between two particles. As the distance is very low, the interparticle force is strongly attractive (at bottom, right down of (A)), the particles are strongly flocculated; as the distance is moderate, the interparticle force is strongly repulsive (at middle, right down of (A)), the particles are dispersed; as the distance is large, the interparticle force is attractive again (at top, right down of (A)), the particles are weakly flocculated. (B) Rheological behaviors of suspensions as steady-shear flow [33] (a) shear rate vs. viscosity; (b) shear rate vs. stress. Curve (1), Newtonian flow; Curve (2), Bingham plastic; Curve (3), shear-thinning; Curve (4), pseudoplastic with yield stress; and Curve (5), shear-thickening. (C) Schematic illustration of oscillatory behavior as a function of frequency [30]. (a) Liquid-like; (b) gel-like; and (c) solid-like. The rheological properties of suspension shown in (B,C) are determined by the interparticle forces shown in (A). Reprinted with permission [30]. Copyright (2000), WILEY-VCH.

The repulsive electrostatic forces depend on two elements: the dielectric properties of the intervening solvent and the magnitude of like-charges at the solid-liquid interface surrounding each particle. The former is determined by the natural properties of the used solvent, which is not prone to control; the latter is more sophisticated and can be adjusted by a few variates. Actually, once a powder is immersed in a solvent such as water, the charges are generated by adsorption or desorption of ionic species in solution such as proton-transfer reactions with the surface hydroxyl groups [29]. These reactions with acid and base can be written as

Acid solution:



Basic solution:



In an acid solution, the surface hydroxyl groups react with hydrogen ion from acids, while in a basic solution, the surface hydroxyl groups react with hydroxyl ions from the

basics. The pH value of the solution plays an important role in the sum of hydrogen or hydroxyl ions in the solvent and then affects the net charge at the particle surface. Reaction activity of the particular material and ions concentration are other factors. Indeed, at one pH, called the isoelectric point ( $pH_{IEP}$ ), the net charge is zero. Therefore, the surface is neutral at  $pH = pH_{IEP}$ , negative at  $pH > pH_{IEP}$ , and positive at  $pH < pH_{IEP}$ . As its surface is charged, counterions, i.e., ions of opposite charge, are assembled around the particle, and a diffuse ion cloud termed the electrical double layer (EDL) is formed adjacent to the particle surface. A high ionic strength (high concentration of ions) results in a thin thickness of EDL. The theory on the relationship between the surface charge and repulsive electrostatic forces is very complicated. Simply, this repulsive force decreases exponentially with surface distance  $D$  and is inversely proportional to the square root of the ionic strength [27,29]. Note that the electrostatic force only existed in aqueous systems.

Combining the vdW attractive force and the electrostatic repulsive forces is the well-known Derjaguin-Landau-Verwey-Overbeek (DLVO) theory [27]. The magnitude of the interaction force between two particles is taken over by the dielectric properties of materials, surface charge, and ionic strength. With less surface charge or higher ionic strength, the repulsive force is lower, and particles are flocculated. Thus, there are two routes to control the states of particles, which take charge of the rheological properties of suspensions (see Section 2.2). One is adjusting the pH value to change the net charge on the particle surfaces; the other is tailoring the ionic strength to change the range of the double-layer repulsion.

Another repulsive force is the steric force stemmed from organic molecules such as dispersants or surfactants adsorbed on the particle surface. An adsorption layer formed takes part in preventing particles from approaching each other and bridging flocculation. The thickness of the adsorption layer, depending on the molecular architecture, anchoring sites, and strength, extending conformation of molecules in the solvent as well as solvent quality [34], should be high enough for generating steric repulsion to overwhelm vdW attractive force. Note that this principle of steric force is effective in aqueous and non-aqueous systems.

Specially, in aqueous systems, if the molecules are polyelectrolytes containing at least one type of ionizable group such as carboxylic or sulfonic acid groups, both electrostatic and steric forces take part in such systems, termed as the electrostatic force. For example, poly(acrylic acid) (PAA), a widely used additive, possesses three ionizable segments. In a suspension with PAA, these electrostatic forces result: the electrostatic force from ionized carboxylic acid groups and the steric force from the polymeric adsorption layer [35–37]. The routes to change the electrostatic and steric forces are certainly useful to change the electrostatic force. For a given system with anionic polyelectrolytes, increasing pH induces the increase of the ionization degree and, correspondingly, the adsorption behavior and the conformation of molecules.

The last force between particles is the depletion force, which is resulted from the presence of small species called depletants [38–40]. These depletants, which are very fine organic molecules [38–41] in free status, can induce stabilization or flocculation of particles. That is, the depletion force is repulsive or attractive.

## 2.2. Rheological Properties of Suspensions

Fundamentally, the rheological properties depend on thermodynamics and fluid mechanics interactions between particles, including Brownian motion, the rheological response, and the suspension structure. Suspensions illustrate two typical rheological behaviors in response to different mechanical loading, i.e., type of stress or strain: viscous behavior to shear flow and viscoelastic behavior to oscillatory flow, as shown in Figure 1B.

Viscous behavior presents in the form that apparent viscosity ( $\eta$ ) is a function of shear stress ( $\tau$ ) and shear rate ( $\dot{\gamma}$ ), which is the result of steady shear on suspension relative to its original composition and structures disturbance during shearing (Figure 1B). When the function is a linear equation passing through the origin of the coordinate axis, the flow of suspension is a Newtonian behavior (curve (1), Figure 1B). In such systems,

the suspension structure is dominated only by thermodynamic Brownian motion and hydrodynamic interactions. If the intercept of this linear equation is above zero, the flow is a Bingham plastic behavior (curve (2), Figure 1B), which shows yield stress. If the viscosity ( $\eta$ ) decreases with shear rate ( $\gamma$ ), the flow is pseudoplastic or shear-thinning behavior (curve (3), Figure 1B) due to the perturbation of the suspension structure [42]. Furthermore, this response can be accompanied by yield stress. The magnitude of this stress depends on the strength of the particle network (curves (2) and (4), Figure 1B). Oppositely, if the viscosity ( $\eta$ ) increases with shear rate ( $\gamma$ ), the flow is dilatant or shear-thickening behavior (curve (5), Figure 1B). With increasing shear rate, the suspension structures undergo transitions either from disorder to order [43] or form stable particles to cluster [44]. The degree of shear-thinning or thickening increases with solids loading ( $\Phi$ , volume fraction of particles).

Viscoelastic behavior is mainly the response of concentrated suspension to oscillatory flow. When a frequency ( $\omega$ )-dependent shear stress or strain is applied, the suspension has a shear modulus. This shear modulus ( $G^*$ ) consists of a storage ( $G'$ ) and a loss modulus ( $G''$ ), as given by Gao and Lewis [30,33], whose papers have more details.

$$G^* = G' + iG'' \quad (3)$$

$$G' = G^* \cos\theta \quad (4)$$

$$G'' = G^* \sin\theta \quad (5)$$

where  $\theta$  is the phase angle. Conducting frequency ( $\omega$ ) sweeps at given stress (or strain), and the suspension shows its viscoelastic behavior accompanied by specific structural information. Over the entire frequency spectrum, as  $G'' > G'$ , the response is liquid-like; as  $G'' < G'$  (independent of frequency), the response is solid-like; a gel-like response is observed when  $G''$  and  $G'$  vary as  $\omega^j$ , where  $j$  is in the range of 0.3–0.7, as shown in Figure 1c.

These rheological properties of suspension, including viscous and viscoelastic behaviors, can be transitioned to each other by tailoring interaction in a given system. For example, in a well-dispersed system, flocculation occurs as the net force between particles turns to be attractive via adjusting pH value, ionic concentration, etc. [15,23,45,46]. Moreover, the average separation distance between particles also strongly plays a role in the inter-particle forces and the fluid mechanics interactions. For example, in a flocculated system, the properties of the concentrated suspension transition drastically at a certain critical solid loading ( $\Phi_g$ ). At  $\Phi_g$ , a space-filling particle network forms. When  $\Phi < \Phi_g$ , the suspension behavior under steady shear is without yield stress, and the discrete clusters in suspension structure settle more or less independently. Above  $\Phi_g$ , the suspension behavior has stress before yielding; the viscoelastic behaviors may be significant, and the rate of settling is very slow [29,30].

### 3. Suspensions for 3D Printing

To meet the requirements of 3D-printing techniques, suspensions should possess a specific suspension structure and rheological property. Note that the suspensions are mostly concentrated, i.e., with high solids loading because of the shape-preserving application in post-treatment processing.

A well-dispersed, stabilized, concentrated suspension is needed for selective laser sintering [9], slurry-based 3D printing [47], and ceramic stereolithography including SLA/DLP [17,48,49]. A strongly flocculated, concentrated suspension is needed for direct ink writing [20,21,23,24,50]. Typically, in the systems for DIW, the transitions of concentrated suspensions from well-dispersed to strongly flocculated with or without assistance are reported. Therefore, to elucidate suspensions for 3D printing, the suspensions for DIW are taken as an example in this section.

### 3.1. Classification of Suspensions for Direct Ink Writing

In the forming process, direct ink writing is firstly carried out using special devices (e.g., nozzles) to form a fluid with a linear shape, termed as characteristic linear fluid. Afterward, the characteristic linear fluid and the inherited characteristics are automatically controlled by a computer. The trajectory of the moving platform of the fluid enables the preparation of predetermined structures with complex components [20]. Clearly, in order to achieve a complex periodic structure with three-dimensional features, the linear fluid has to become rapid (loss of flow) after it has left a special device. So linear fluids can be classified into two categories based on the curing of the fluid as it loses its fluidity: I. self-solidification route; II. assistant-solidification route.

### 3.2. Self-Solidification Route

#### 3.2.1. Requirements and Mode for Self-Solidification Suspension

Direct ink writing places high demands on self-solidification suspensions. It requires that the suspension be able to pass smoothly through a nozzle to form a fluid with a linear shape, and it retains its shape in a fast-curing manner. Moreover, the assembled overhanging beam structure does not buckle or collapse. In terms of rheological properties, the suspensions must fulfill four basic requirements [20,23]:

- (1) Low viscosity under high shear rate. This enables suspensions' smooth passage through the nozzle without clogging.
- (2) Loss of fluidity under non-shear conditions. This means that the linear fluid must cure quickly and solidify after passing through the nozzle.
- (3) Good elastic properties such as high storage modulus after curing for keeping the shape linear.
- (4) High solids loading. In follow-up procedures such as drying (or sintering), deformation and cracking of the formed three-dimensional complex structures can be avoided.

#### 3.2.2. Rheological Properties of the Suspensions

In the printing process, the surface of the fluid with linear shape would flow under shear frictional forces with the inner walls of the nozzle, while the suspension inside retains its gel properties and hardly flows. Therefore, the structure of the linear fluid regard as a nucleus (rigid gel state)-shell (shear flow dynamic) structure [23]. The rheological properties are well suited to the Herschel–Bulkley model (curve (4), Figure 1B):

$$\tau = \tau_y + K\dot{\gamma}^n \quad (6)$$

where  $\tau$  is the shear stress,  $\tau_y$  is the shear yield stress,  $K$  is the viscosity index,  $n$  is the shear-thinning index, and  $\dot{\gamma}$  is the shear rate. When the shear stress ( $\tau$ ) on the suspension is higher than the shear yield stress ( $\tau_y$ ), the linkage between the particles is broken, and the surface suspension can flow. In order to avoid pressure filtration [23], the shear stress ( $\tau$ ) must be lower than the compressive yield stress ( $P_y$ ) of the suspension. It is, therefore, possible that the range of shear stresses to be applied should be as follows:

$$\tau_y < \tau < p_y \quad (7)$$

#### 3.2.3. Elastic Properties of the Suspensions

When the characteristic linear fluid is no longer subjected to shear stress after exiting the pore of the nozzle, the linking between the particles within the shear flow dynamic shell reoccurs, and the suspension transforms into a rigid gel state, thus serving the same purpose as a rigid gel state nucleus. The elastic properties of the gel state can be expressed by the following equation [51,52]:

$$y = k \left( \frac{\Phi}{\Phi_{gel}} - 1 \right)^x \quad (8)$$

where  $y$  is the elastic properties of the suspension (including the shear yield stress  $\tau_y$  and the storage modulus  $G'$ ),  $k$  is a constant,  $\Phi_g$  is the solids loading corresponding to the critical point of the gel, and  $x$  is the proportionality constant (generally around 2.5). It can be seen that the elastic properties of the gel are mainly determined by two parameters: the solids loading ( $\Phi$ ) and the gel point solids loading ( $\Phi_g$ ). As the solids loading increases, the density of interparticle linking bonds in the suspension increases, and the elastic properties rise. The opposite effect is seen with gel solids loading, where an increase in gel solids loading decreases the strength of the link bonds and hence the elastic properties. Therefore, in order to meet the requirements of straight-write forming, the elastic properties of colloidal suspensions can be achieved by adjusting the solids loading ( $\Phi$ ) and the gel point solids loading ( $\Phi_g$ ).

### 3.2.4. Design Guidelines for Self-Solidification Suspensions

The rheological properties of self-solidification suspensions (colloidal gel suspensions) are determined by three parameters: the stress ( $\sigma$ ), the solids loading ( $\Phi$ ), and the interparticle attraction energy ( $U$ ), as the report by V. Trappe [53]. The stress on the suspension has an effect on the network structure, consisted of particles formed by the interparticle attraction, and the critical solid-phase volume fraction increases with increasing stress. The interparticle interaction within the suspension, influenced by a number of factors, including  $\sigma$ ,  $\Phi$ , and  $U$ , can be easily modulated by changing these factors so as to achieve a self-solidification suspension that meets the requirements of direct ink writing.

### 3.2.5. Typical Self-Solidification Suspensions

The self-solidification suspensions currently used are colloidal suspensions whose rheological properties are controlled by some routes, mainly colloidal gel suspensions and biphasic suspensions, as listed in Table 1 [15,23,45,54–56]. For the colloidal gel suspensions, it is the flocculation of colloidal particles in a flowing suspension that reduces the volume fraction of the solid phase at the gel point of the suspension, increases the elastic properties of the suspension, and ultimately forms a gelatinous colloidal suspension. Smay et al. [23] designed colloidal gel suspensions, i.e., suspensions in which colloidal particles are flocculated and interlinked in a solvent. They first prepared stable and dispersed colloidal suspensions and then, by changing the pH of the suspension, caused the colloidal particles to aggregate. Similarly, colloidal gel suspensions can be obtained by changing the ionic concentration of the suspension [45] or by adding a counter-ionic polyelectrolyte [46]. Graule et al. [57] studied the effect of pH and salt concentration on the state of  $\text{Al}_2\text{O}_3$  suspensions, and Rhodes et al. [58] used a confocal laser scanning microscope to observe homopolymer polyelectrolytes (poly(trimethylammonium iodide), poly(trimethylammonium iodide), poly(trimethylammonium iodide), poly(trimethylammonium iodide), and poly(trimethylammonium iodide) at different pH and salt concentrations. The microscopic structure of silica suspensions dispersed by the polymers (ethylmethacrylate, PTMAM) was found to increase the flocculation of homopolymer-dispersed suspensions with increasing pH and salt concentrations. In addition, pH and salt concentration, as well as the addition of counter-ionic polyelectrolytes, can reduce the volume fraction of the solid phase at the gel point ( $\Phi_g$ ). Smay et al. [23] formed a three-dimensional structure of PZT (Lead zirconate titanate) by varying the pH of the colloidal suspension.

**Table 1.** Self-solidification suspensions designed for direct ink writing [15,23,45,54–56].

Self-Solidification Suspensions	Tailoring Routes for Rheological Properties of Suspensions	Minimum Feature Size in 3D Structures	References
Colloidal gel suspensions	Changing pH values	100 $\mu\text{m}$	[15,23,55]
	Tailoring ionic concentrations	30 $\mu\text{m}$	[45]
	Adding oppositive polyelectrolyte	100 $\mu\text{m}$	[54]
Biphasic suspensions	Changing inter environment of suspensions with homopolymer and copolymer, e.g., ionic concentrations	<100 $\mu\text{m}$	[56]
	Controlling the hydrophilicity/hydrophobicity between particles and solvent	-	[56]
	Using powder with different isoelectric points (IEP)	-	[56]

For the biphasic suspensions, there are three routes to obtain:

- (1) Two types of dispersed biphasic suspensions. This is achieved by taking advantage of the different sensitivities of homopolymer and copolymer polyelectrolyte dispersants to factors such as ionic strength. Firstly, two stable suspensions are prepared using a homopolymeric dispersant (e.g., PAA) and a copolymeric dispersant (e.g., PAA-PEO), respectively. Then, mix them evenly. Finally, the ionic strength of the suspensions was increased [56], or a counter-ionic polyelectrolyte [53] was added to flocculate the colloidal particles of the homopolymeric dispersant while the colloidal particles of the copolymeric dispersant remained stably dispersed regardless of the changing conditions.
- (2) Hydrophilic biphasic suspensions. These suspensions are achieved by modulating the hydrophilicity (polarity) of the hydrophilic colloidal particles, the hydrophobic colloidal particles, and the solvent. For example, with hydrophilic substances (e.g., water) as Jennifer et al. [56] studied amphiphilic biphasic suspensions of  $\text{SiO}_2$ , where the hydrophobic  $\text{SiO}_2$  was obtained by surface modification.
- (3) Isoelectric point biphasic suspensions. The two particles with different isoelectric points were combined to form a biphasic suspension of  $\text{SiO}_2$ . Soluble particles mixed with the same environment (pH, ionic strength, and concentration of dispersant) can be used in a wide range of applications. In the agent, one of the particles is attracted to the other by van der Waals forces and then flocculation. The other particles are subject to electrostatic and steric repulsion [56].

### 3.3. Assistant-Solidification Route

#### 3.3.1. Requirements and Mode for Assistant-Solidification Suspension

In the same way as self-solidification suspensions, assistant-solidification suspensions also require four characteristics to ensure smooth implementation of direct writing:

- (1) Low viscosity when passing through the nozzle;
- (2) Rapid curing under certain external conditions after passing through the nozzle;
- (3) Good elastic properties of the cured linear features;
- (4) A high-volume fraction of the solid phase in the suspension.

Of these, the first and fourth points are easier to achieve. Since externally cured suspensions do not rely on a change in their rheological properties to solidify, stable and dispersed suspensions are generally able to meet the above requirements. The third point is mainly influenced by the curing effect of the second point; therefore, the design and control of the curing action conditions in the second point is the key to its formation.



### 3.3.2. Typical Assistant-Solidify Suspensions

Current curing conditions for externally cured suspensions in direct ink writing can be divided into three main types: solvent evaporation, solubility differences, and UV-curing, as listed in Table 2.

**Table 2.** Assistant-solidification suspensions designed for direct ink writing.

External Conditions for Solidification of Suspensions	Assistant-Solidification Suspensions	Minimum Feature Size in 3D Structures	References
Fast evaporation of solvent in suspensions	Colloidal suspensions with shear-thinning behavior	500 $\mu\text{m}$ 410 $\mu\text{m}$	[21] [24]
	Suspensions composed of nanoparticles and organic solvent	1 $\mu\text{m}$	[50,59]
Solubility divergence between solvent in suspensions and liquid in deposition reservoir	Polyelectrolyte complexes (PECs)	500 30 1	[22,50,60]
Polymerization of organic monomer under ultraviolet irradiation	Silk fibroin solution	5 $\mu\text{m}$	[61]
	Sol-gel suspension	0.3 $\mu\text{m}$	[62]
	Organic monomer solution	5 $\mu\text{m}$	[63]
	Suspensions containing organic monomer	-	[64]
Thermosetting components solidify faster under the influence of temperature The hydrophobic components solidify in water	Organic sulfate suspension	150 $\mu\text{m}$	[65]
	Alumina composite suspension	400 $\mu\text{m}$	[66]
	Preceramic polymer suspension	200 $\mu\text{m}$	[67]

For solvent evaporation, suspensions are nanoparticle-containing suspensions prepared with organic solvents (referred to as nanoparticle/organic solvent suspensions). The suspensions contain solid particles of nanoscale size and a high boiling organic solvent with the function of absorbing water. As a result, the characteristic size of the three-dimensional structures prepared with such suspensions is very small, even down to the nanoscale. The suspension would rapidly obtain solvent evaporation when the specific surface area of linear fluids is very large. Here, the solvent evaporates rapidly, and the rheological properties of the suspension change dramatically. Ahn et al. [50,63] prepared three-dimensional structures with a minimum feature size of 1  $\mu\text{m}$  (high aspect ratio above 6) using a nanosilver/glycol suspension. They used silver nitrate as a precursor, polyacrylic acid as a dispersant, and diethanolamine as a reducing agent to obtain silver particles of around 5 nm with vigorous stirring, then added ethanol to precipitate the polyacrylic acid from the water and coat the silver particles. The suspension can be used to prepare flexible microelectrodes with a cantilevered frame structure, which is of great importance for three-dimensional encapsulation in the field of electronic packaging. Duoss et al. [62] have designed a new sol-gel suspension. They used anhydrous ethanol as a solvent and acetylacetonate-disopropoxytitanium as a precursor to convert the solvent from a sol to a gel by hydrolysis and condensation of metal-alcohol salts at 80 °C. The solvent was then solidified by volatilization of the organic solvent. In practice, the suspension is an organometallic salt gel solution with no suspended solid particles, which makes it easy to pass through the micropores of the pinhead and yields a periodic structure with a small minimum characteristic size. Duoss et al. [62] formed a three-dimensional periodic structure that is flat and uniform in size with a minimum feature size of approximately 0.3  $\mu\text{m}$ . Ahn et al. [68] designed a sol-gel suspension that can be used to prepare ITO (tin-doped indium oxide) microelectrodes by adding indium acetate and acetylacetonate to tin chloride in acetylacetonate and oxidizing it with tetramethylammonium hydroxide and hydrogen peroxide to obtain an ITO sol-gel suspension.

In terms of solubility differences, solidity can also be achieved by taking advantage of the difference in solubility of the suspension, especially of organic substances. In the process, a reservoir containing the fluid in which the solubility of the substance is very low

is placed underneath the printing nozzle. As soon as the suspension emerges from the tip of the printing nozzle, the linear fluid loses its fluidity and becomes more elastic as it enters the sedimentation cell, thus being able to retain its shape. Polyelectrolyte complexes, polyelectrolyte complexes (PECs), for example, is a mixture of two transparent aqueous solutions of polyelectrolytes with opposite charges, which are electrostatically attracted to each other and precipitate out to form a turbid suspension, with the precipitates rapidly aggregating in some liquids without dispersion [69]. Gratson et al. [60] used a suspension of a polyelectrolyte mixture consisting of polyacrylic acid and polyethyleneimine (PAA-PEI) for direct ink writing. They placed a sedimentation cell with an aqueous isopropanol solution beneath the nozzle to allow rapid solidification of the characteristic linear fluid directly into the cell. The phase behavior, rheological properties, and direct ink writing of the polyelectrolyte mixture suspensions were systematically studied [50]. Figure 2 shows a schematic illustration of straightforward modeling using a sedimentation cell [22]. Their study also showed that the concentration of the aqueous isopropanol solution had an effect on the solidification mechanism of the characteristic linear fluid of the polyelectrolyte suspension. Xu et al. [22] also studied polyelectrolyte suspensions consisting of polyacrylic acid and polyallyl chlorinated amine (PAA-PAH) and obtained similar results. Ghosh et al. [61] used fibrous protein solutions for direct writing, taking advantage of the insolubility of fibrous protein solutions in aqueous methanol and the weight that rapid precipitates can support to obtain three-dimensional stacked structures with a characteristic size of 5  $\mu\text{m}$ . The optimal liquid composition of the deposition cell is an 86% aqueous methanol solution.

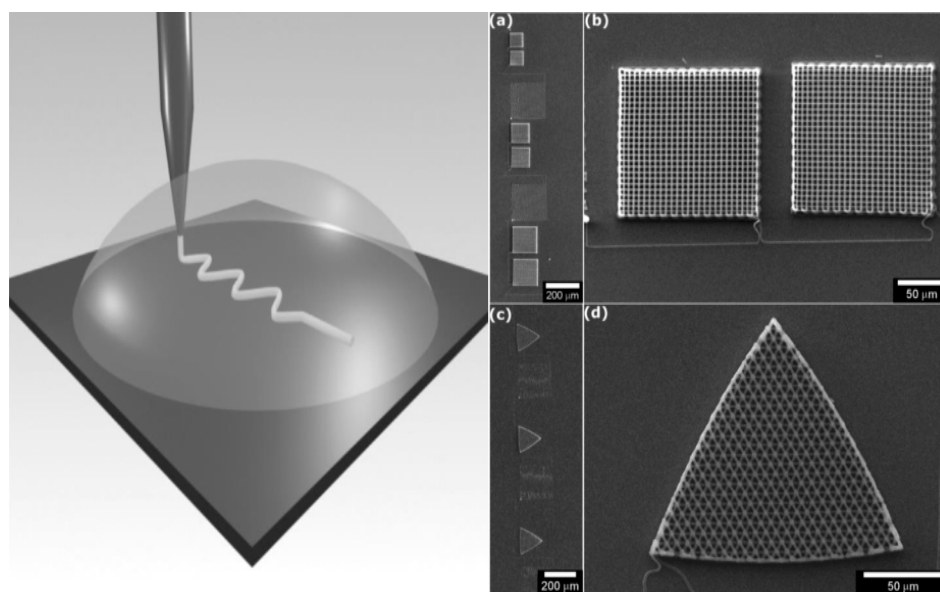


**Figure 2.** Direct ink writing of three-dimensional microperiodic structure Reprinted with permission [22]. Copyright (2007) American Chemical Society.

For the UV-curing, the printing materials contain some photosensitive substances to achieve UV-curing. Sun et al. [18,70] used methyl methacrylate as the monomer, pentaerythritol tripropionate as the crosslinker, and 2,2-diethoxyacetophenone as the photoinitiator to prepare a light-curable suspension of  $\text{BaTiO}_3$ , and prepared three-dimensional structures with a characteristic size of 0.4 mm on a dispensing system equipped with a UV light source. Barry et al. [31] also used the same principle to prepare three-dimensional hydrogel buildup structures for cell growth control. Wei et al. [71] applied UV-curing to the printing separator and packaging ink of LIB (Lithium-Ion Battery) by adding UV-curing epoxy resins.

For consolidation by heating, the print material is consolidated faster by increasing or decreasing the temperature of the plate or atmosphere. Unlike the route of solvent

evaporation, a change in temperature speeds up the solidification process rather than converting it into a gel. Yang et al. [66] add carrageenan swelling and ammonium citrate as thermosetting agents into the alumina powder. In this printing, upon the atmosphere and flat panels being heated, the viscosity of the suspension increased to a degree for the solidification.

#### 4. Perspective

3D printing is a rapidly growing manufacturing technology for the fabrication of three-dimensional objects, which has been used in the fields of microelectronics packaging, lithium-ion batteries, photonic crystals, soft robot, metamaterials, and biomedical materials. As a sophisticated printing material, more and more suspensions for 3D printing are being proposed. From the point of view of the authors, the directions developing the suspensions are outlined as follows:

- (1) Optimizing the ways to change the interaction between particles. As aforementioned, the rheological properties of suspension for the self-consolidation in direct ink writing can be adjusted. However, the range of technical parameters is narrow, and its rheological properties are difficult to be well controlled. Thus, the routes to control the interaction in the suspensions for 3D printing should be optimized.
- (2) Developing functional particles via surface modification. Functional particles suspending in a solvent can be used to control the suspension properties or to promote printing. For example, the suspensions of particles covered by stimulus-responsive species can be tailored by thermal, magnetic, or electric fields; the suspensions of particles coated by an organic with functional groups benefit polymerization, and 3D printing processing will be easier and more stable.
- (3) Developing specific suspensions for novel 3D-printing techniques. Recently, several 3D-printing techniques have been reported for high-speed printing such as continuous liquid interface production (CLIP) [72,73]. A dead layer created by polymerization inhibition of oxygen or a fluorinated oil is used to undergo continuous liquid interface printing, and this continuous printing approach increases vertical print speeds by two orders of magnitude. However, these techniques are based on special materials. Therefore, to embrace the novel 3D-printing techniques, specific suspensions should be developed to meet the printing needs.

**Author Contributions:** Author Contributions: H.Z.; X.W. (Xiaofeng Wang) and X.W. (Xinyu Wang) conceived the idea, reviewed the literature, wrote the manuscript; C.P. and R.W. revised the content, wrote the manuscript; X.W. (Xiaofeng Wang) and K.Z. conceived the idea, reviewed the literature, wrote the manuscript. All authors have read and agreed to the published version of the manuscript.

**Funding:** The research was funded by the joint funding between The Hebrew University (HU) and Central South University (CSU), HUCNN-CSU-2019, and by the Natural Science Foundation of Hunan Province, China (No. 2020JJ4729).

**Institutional Review Board Statement:** Not applicable.

**Informed Consent Statement:** Not applicable.

**Data Availability Statement:** No data was generated.

**Conflicts of Interest:** The authors declare no conflict of interest.

#### References

1. Gibson, I.; Rosen, D.W.; Stucker, B. *Additive Manufacturing Technologies*; Springer: New York, NY, USA, 2015.
2. Ngo, T.D.; Kashani, A.; Imbalzano, G.; Nguyen, K.T.Q.; Hui, D. Additive manufacturing (3D printing): A review of materials, methods, applications and challenges. *Compos. Part B Eng.* **2018**, *143*, 172–196. [[CrossRef](#)]
3. Prakash, K.S.; Nancharaih, T.; Rao, V.S. Additive Manufacturing Techniques in Manufacturing An Overview. *Mater. Today Proc.* **2018**, *5*, 3873–3882. [[CrossRef](#)]

4. DebRoy, T.; Wei, H.L.; Zuback, J.S.; Mukherjee, T.; Elmer, J.W.; Milewski, J.O.; Beese, A.M.; Wilson-Heid, A.D.; De, A.; Zhang, W. Additive manufacturing of metallic components—Process, structure and properties. *Prog. Mater. Sci.* **2018**, *92*, 112–224. [[CrossRef](#)]
5. Layani, M.; Wang, X.; Magdassi, S. Novel Materials for 3D Printing by Photopolymerization. *Adv. Mater.* **2018**, *30*, e1706344. [[CrossRef](#)]
6. Galante, R.; Figueiredo-Pina, C.G.; Serro, A.P. Additive manufacturing of ceramics for dental applications: A review. *Dent. Mater.* **2019**, *35*, 825–846. [[CrossRef](#)] [[PubMed](#)]
7. Yap, Y.L.; Sing, S.L.; Yeong, W.Y. A review of 3D printing processes and materials for soft robotics. *Rapid Prototyp. J.* **2020**, *26*, 1345–1361. [[CrossRef](#)]
8. Goh, G.D.; Yap, Y.L.; Tan, H.K.J.; Sing, S.L.; Goh, G.L.; Yeong, W.Y. Process–Structure–Properties in Polymer Additive Manufacturing via Material Extrusion: A Review. *CRC Crit. Rev. Solid State Sci.* **2020**, *45*, 113–133. [[CrossRef](#)]
9. Tang, H.-H.; Chiu, M.-L.; Yen, H.-C. Slurry-based selective laser sintering of polymer-coated ceramic powders to fabricate high strength alumina parts. *J. Eur. Ceram. Soc.* **2011**, *31*, 1383–1388. [[CrossRef](#)]
10. Brady, G.A.; Halloran, J.W. Solid Freeform Fabrication of Ceramics by Stereolithography. *J. Am. Ceram. Soc.* **1996**, *79*, 2601–2608.
11. Chartier, T.; Badev, A.; Abouliatim, Y.; Lebaudy, P.; Lecamp, L. Stereolithography process: Influence of the rheology of silica suspensions and of the medium on polymerization kinetics—Cured depth and width. *J. Eur. Ceram. Soc.* **2012**, *32*, 1625–1634. [[CrossRef](#)]
12. Wang, Y.Y.; Li, L.; Wang, Z.Y.; Liu, F.T.; Zhao, J.H.; Zhang, P.P.; Lu, C. Fabrication of Dense Silica Ceramics through a Stereo Lithography-Based Additive Manufacturing. *Solid State Phenom.* **2018**, *281*, 456–462. [[CrossRef](#)]
13. Liu, C.; Qian, B.; Liu, X.; Tong, L.; Qiu, J. Additive manufacturing of silica glass using laser stereolithography with a top-down approach and fast debinding. *RSC Adv.* **2018**, *8*, 16344–16348. [[CrossRef](#)]
14. Azarmi, F.; Amiri, A. Microstructural evolution during fabrication of alumina via laser stereolithography technique. *Ceram. Int.* **2019**, *45*, 271–278. [[CrossRef](#)]
15. Smay, J.E.; Cesarano, J.; Tuttle, B.A.; Lewis, J.A. Piezoelectric properties of 3-X periodic Pb(ZrxTi1-x)O-3-polymer composites. *J. Appl. Phys.* **2002**, *92*, 6119–6127. [[CrossRef](#)]
16. Wang, Y.; Wang, Z.; Liu, S.; Qu, Z.; Han, Z.; Liu, F.; Li, L. Additive manufacturing of silica ceramics from aqueous acrylamide based suspension. *Ceram. Int.* **2019**, *45*, 21328–21332. [[CrossRef](#)]
17. Zhou, W.; Li, D.; Wang, H. A novel aqueous ceramic suspension for ceramic stereolithography. *Rapid Prototyp. J.* **2010**, *16*, 29–35. [[CrossRef](#)]
18. Sun, J.; Binner, J.; Bai, J. Effect of surface treatment on the dispersion of nano zirconia particles in non-aqueous suspensions for stereolithography. *J. Eur. Ceram. Soc.* **2019**, *39*, 1660–1667. [[CrossRef](#)]
19. Guillaume, O.; Geven, M.A.; Sprecher, C.M.; Stadelmann, V.A.; Grijpma, D.W.; Tang, T.T.; Qin, L.; Lai, Y.; Alini, M.; de Bruijn, J.D.; et al. Surface-enrichment with hydroxyapatite nanoparticles in stereolithography-fabricated composite polymer scaffolds promotes bone repair. *Acta Biomater.* **2017**, *54*, 386–398. [[CrossRef](#)]
20. Lewis, J.A. Direct Ink Writing of Three-Dimensional Ceramic Structures. *J. Am. Ceram. Soc.* **2006**, *89*, 3599–3609. [[CrossRef](#)]
21. Cesarano, J. A Review of Robocasting Technology. *MRS Proc.* **2011**, *542*, 133–139. [[CrossRef](#)]
22. Xu, M.; Lewis, J.A. Phase Behavior and Rheological Properties of Polyamine-Rich Complexes for Direct-Write Assembly. *Langmuir* **2007**, *23*, 12752–12759. [[CrossRef](#)]
23. Smay, J.E.; Cesarano, J.; Lewis, J.A. Colloidal Inks for Directed Assembly of 3-D Periodic Structures. *Langmuir* **2002**, *18*, 5429–5437. [[CrossRef](#)]
24. Zhao, S.; Siqueira, G.; Drdova, S.; Norris, D.; Ubert, C.; Bonnin, A.; Galmarini, S.; Ganobjak, M.; Pan, Z.; Brunner, S.; et al. Additive manufacturing of silica aerogels. *Nature* **2020**, *584*, 387–392. [[CrossRef](#)]
25. Prasad, S. A review of: “INTRODUCTION TO THE PRINCIPLES OF CERAMIC PROCESSING” James S. Reed John Wiley & Sons, New York, NY 485 pages, hardcover. *Mater. Manuf. Process.* **1990**, *5*, 133–134. [[CrossRef](#)]
26. Lunge, F.F. Powder Processing Science and Technology for Increased Reliability. *J. Am. Ceram. Soc.* **2010**, *72*, 3–15. [[CrossRef](#)]
27. Hunter, R.J. Foundations of Colloid Science. *Colloids Surf. A Physicochem. Eng. Asp.* **2002**, *210*, 125.
28. Hartmann, U. Intermolecular and surface forces in noncontact scanning force microscopy. *Ultramicroscopy* **1992**, *42*, 59–65. [[CrossRef](#)]
29. Sigmund, W.M.; Bell, N.S.; Bergström, L. Novel Powder-Processing Methods for Advanced Ceramics. *J. Am. Ceram. Soc.* **2000**, *83*, 1557–1574. [[CrossRef](#)]
30. Lewis, J.A. Colloidal processing of ceramics. *J. Am. Ceram. Soc.* **2000**, *83*, 2341–2359. [[CrossRef](#)]
31. Jones, D.A.R.; Leary, B.; Boger, A.D.V. The rheology of a concentrated colloidal suspension of hard spheres. *J. Colloid Interface Sci.* **1991**, *147*, 479–495. [[CrossRef](#)]
32. De Hek, H.; Vrij, A. Interactions in mixtures of colloidal silica spheres and polystyrene molecules in cyclohexane. *J. Colloid Interface Sci.* **1981**, *84*, 409–422. [[CrossRef](#)]
33. Gao, L.; Sun, J.; Liu, Y.-Q. *Dispersion and Surface Modification of Nano-Powders*; Chemical Industry Press: Beijing, China, 2003. (In Chinese)
34. Napper, D.H. *Polymeric Stabilization of Colloidal Dispersions*; Academic Press: London, UK, 1985; p. 30.

35. Cesarano, J.; Aksay, I.A. Stability of Aqueous  $\alpha$ -Al<sub>2</sub>O<sub>3</sub> Suspensions with Poly(methacrylic acid) Polyelectrolyte. *J. Am. Ceram. Soc.* **1988**, *71*, 250–255. [[CrossRef](#)]
36. Biggs, S.; Healy, T.W. Electrosteric stabilisation of colloidal zirconia with low-molecular-weight polyacrylic acid. An atomic force microscopy study. *J. Chem. Soc. Faraday Trans.* **1994**, *90*, 3415–3421. [[CrossRef](#)]
37. Rojas, O.J.; Claesson, P.M.; Muller, D.; Neuman, R.D. The Effect of Salt Concentration on Adsorption of Low-Charge-Density Polyelectrolytes and Interactions between Polyelectrolyte-Coated Surfaces. *J. Colloid Interface* **1998**, *205*, 77–88. [[CrossRef](#)]
38. Walz, J.Y.; Sharma, A. Effect of Long Range Interactions on the Depletion Force between Colloidal Particles. *J. Colloid Interface Sci.* **1994**, *168*, 485–496. [[CrossRef](#)]
39. Mao, Y. Depletion Force in Polydisperse Systems. *J. Phys. II Fr.* **1995**, *5*, 1761–1766. [[CrossRef](#)]
40. Richetti, P.; Kekicheff, P. Direct measurement of depletion and structural forces in a micellar system. *Phys. Rev. Lett.* **1992**, *68*, 1951–1954. [[CrossRef](#)]
41. Tohver, V.; Smay, J.E.; Braem, A.; Braun, P.V.; Lewis, J.A. Nanoparticle halos: A new colloid stabilization mechanism. *Proc. Natl. Acad. Sci. USA* **2001**, *98*, 8950–8954. [[CrossRef](#)]
42. Bergström, L. Shear thinning and shear thickening of concentrated ceramic suspensions. *Colloids Surf. A* **1998**, *133*, 151–155. [[CrossRef](#)]
43. Marshall, L.; Zukoski, C.F. Experimental studies on the rheology of hard-sphere suspensions near the glass transition. *J. Phys. Chem.* **1990**, *94*, 1164–1171. [[CrossRef](#)]
44. Bender, J.; Wagner, N.J. Reversible shear thickening in monodisperse and bidisperse colloidal dispersions. *J. Rheol.* **1996**, *40*, 899–916. [[CrossRef](#)]
45. Li, Q.; Lewis, J.A. Nanoparticle Inks for Directed Assembly of Three-Dimensional Periodic Structures. *Adv. Mater.* **2003**, *15*, 1639–1643. [[CrossRef](#)]
46. Rao, R.B.; Krafcik, K.L.; Morales, A.M.; Lewis, J.A. Microfabricated Deposition Nozzles for Direct-Write Assembly of Three-Dimensional Periodic Structures. *Adv. Mater.* **2005**, *17*, 289–293. [[CrossRef](#)]
47. Grau, J.; Moon, J.; Uhland, S.; Cima, M.; Sachs, E. High green density ceramic components fabricated by the slurry-based 3DP process. In Proceedings of the International Solid Freeform Fabrication Symposium, Austin, TX, USA, 11–13 August 1997.
48. Hinczewski, C.; Corbel, S.; Chartier, T. Ceramic suspensions suitable for stereolithography. *J. Eur. Ceram. Soc.* **1998**, *18*, 583–590. [[CrossRef](#)]
49. Chartier, T.; Duterte, C. Fabrication of Millimeter Wave Components Via Ceramic Stereo- and Microstereolithography Processes. *J. Am. Ceram. Soc.* **2008**, *91*, 2469–2474. [[CrossRef](#)]
50. Gratson, G.M.; Lewis, J.A. Phase Behavior and Rheological Properties of Polyelectrolyte Inks for Direct-Write Assembly. *Langmuir* **2005**, *21*, 457–464. [[CrossRef](#)] [[PubMed](#)]
51. Li, Q.; Li, B.; Zhou, J.; Li, L.T.; Gui, Z.L. Robocasting: A novel avenue for engineering complex 3D structures. *J. Inorg. Mater.* **2005**, *20*, 13–20.
52. Channell, G.M.; Zukoski, C.F. Shear and compressive rheology of aggregated alumina suspensions. *AIChE J.* **1997**, *43*, 1700–1708. [[CrossRef](#)]
53. Trappe, V.; Prasad, V.; Cipelletti, L.; Segre, P.N.; Weitz, D.A. Jamming phase diagram for attractive particles. *Nature* **2001**, *411*, 772–775. [[CrossRef](#)]
54. Sun, Q.; Liu, J.; Cheng, H.; Mou, Y.; Liu, J.; Peng, Y.; Chen, M. Fabrication of 3D structures via direct ink writing of kaolin/graphene oxide composite suspensions at ambient temperature. *Ceram. Int.* **2019**, *45*, 18972–18979. [[CrossRef](#)]
55. Smay, J.E.; Cesarano, J.; Tuttle, B.A.; Lewis, J.A. Directed Colloidal Assembly of Linear and Annular Lead Zirconate Titanate Arrays. *J. Am. Ceram. Soc.* **2004**, *87*, 293–295. [[CrossRef](#)]
56. Lewis, J.A.; Li, Q.; Rao, R. Biphasic Inks. U.S. Patent 8187500, 29 May 2012.
57. Graule, T.J.; Gauckler, L.J.; Baader, F.H. Direct coagulation casting—A new green shaping technique Part I. Processing principles. *Ind. Ceram.* **1996**, *16*, 31–34.
58. Rhodes, S.K.; Lambeth, R.H.; Gonzales, J.; Moore, J.S.; Lewis, J.A. Cationic Comb Polymer Superdispersants for Colloidal Silica Suspensions. *Langmuir* **2009**, *25*, 6787–6792. [[CrossRef](#)]
59. Ahn, B.Y.; Duoss, E.B.; Motala, M.J.; Guo, X.; Park, S.I.; Xiong, Y.; Yoon, J.; Nuzzo, R.G.; Rogers, J.A.; Lewis, J.A. Omnidirectional printing of flexible, stretchable, and spanning silver microelectrodes. *Science* **2009**, *323*, 1590–1593. [[CrossRef](#)]
60. Xu, M.; Lewis, J.A. Microperiodic structures: Direct writing of three-dimensional webs. *Nature* **2004**, *428*, 386. [[CrossRef](#)]
61. Ghosh, S.; Parker, S.T.; Wang, X.; Kaplan, D.L.; Lewis, J.A. Direct-Write Assembly of Microperiodic Silk Fibroin Scaffolds for Tissue Engineering Applications. *Adv. Funct. Mater.* **2008**, *18*, 1883–1889. [[CrossRef](#)]
62. Duoss, E.B.; Twardowski, M.; Lewis, J.A. Sol-Gel Inks for Direct-Write Assembly of Functional Oxides. *Adv. Mater.* **2007**, *19*, 3485–3489. [[CrossRef](#)]
63. Barry, R.A.; Shepherd, R.F.; Hanson, J.N.; Nuzzo, R.G.; Wiltzius, P.; Lewis, J.A. Direct-Write Assembly of 3D Hydrogel Scaffolds for Guided Cell Growth. *Adv. Mater.* **2009**, *21*, 2407–2410. [[CrossRef](#)]
64. Shepherd, R.F.; Panda, P.; Bao, Z.; Sandhage, K.H.; Hatton, T.A.; Lewis, J.A.; Doyle, P.S. Stop-Flow Lithography of Colloidal, Glass, and Silicon Microcomponents. *Adv. Mater.* **2008**, *20*, 4734–4739. [[CrossRef](#)]
65. Mariani, L.M.; Johnson, W.R.; Considine, J.M.; Turner, K.T. Printing and mechanical characterization of cellulose nanofibril materials. *Cellulose* **2019**, *26*, 2639–2651. [[CrossRef](#)]

66. Yang, L.; Zeng, X.; Ditta, A.; Feng, B.; Su, L.; Zhang, Y. Preliminary 3D printing of large inclined-shaped alumina ceramic parts by direct ink writing. *J. Adv. Ceram.* **2020**, *9*, 312–319. [[CrossRef](#)]
67. Pierin, G.; Grotta, C.; Colombo, P.; Mattevi, C. Direct Ink Writing of micrometric SiOC ceramic structures using a preceramic polymer. *J. Eur. Ceram. Soc.* **2016**, *36*, 1589–1594. [[CrossRef](#)]
68. Ahn, B.Y.; Lorang, D.J.; Duoss, E.B.; Lewis, J.A. Direct-write assembly of microperiodic planar and spanning ITO microelectrodes. *Chem. Commun.* **2010**, *46*, 7118–7120. [[CrossRef](#)]
69. Philipp, B.; Dautzenberg, H.; Linow, K.-J.; Kötz, J.; Dawydoff, W. Polyelectrolyte complexes—Recent developments and open problems. *Prog. Polym. Sci.* **1989**, *14*, 91–172. [[CrossRef](#)]
70. Sun, J.-B.; Li, B.; Cai, K.-P.; Zhou, J.; Li, L.-T. TiO<sub>2</sub> Photolysis Device Fabricated by Direct Ink Write Assembly. *J. Inorg. Mater.* **2011**, *26*, 300–304. [[CrossRef](#)]
71. Wei, T.-S.; Ahn, B.Y.; Grotto, J.; Lewis, J.A. 3D Printing of Customized Li-Ion Batteries with Thick Electrodes. *Adv. Mater.* **2018**, *30*, e1703027. [[CrossRef](#)]
72. Tumbleston, J.R.; Shirvanyants, D.; Ermoshkin, N.; Januszewicz, R.; Johnson, A.R.; Kelly, D.; Chen, K.; Pinschmidt, R.; Rolland, J.P.; Ermoshkin, A.; et al. Continuous liquid interface production of 3D objects. *Science* **2015**, *347*, 1349–1352. [[CrossRef](#)] [[PubMed](#)]
73. Walker, D.A.; Hedrick, J.L.; Mirkin, C.A. Rapid, large-volume, thermally controlled 3D printing using a mobile liquid interface. *Science* **2019**, *366*, 360–364. [[CrossRef](#)]